Normal and shear stresses on a residual limb in a prosthetic socket during ambulation: Comparison of finite element results with experimental measurements

Joan E. Sanders, PhD and Colin H. Daly, PhD
Center for Bioengineering and Department of Mechanical Engineering, University of Washington, Seattle, WA 98195; Prosthetics Research Study, Seattle, WA 98122

Abstract—Interface stresses on a below-knee amputee residual limb during the stance phase of gait calculated using an analytical finite element model were compared with experimental interface stress measurements. The model was quasi-static and linear. Qualitatively, shapes of analytical and experimental interface stress waveforms were similar in that they were double-peaked with some distinct features apparent. However, quantitatively analytical resultant shear stress magnitudes were less than experimental values at all transducer measurement sites. Analytical normal stresses were less than experimental values at postero-proximal, postero-distal, and antero-medial proximal sites, but were greater than experimental values at antero-lateral distal and antero-lateral proximal sites. Anterior resultant shear angles were directed more distally in the model than in clinical data, an expected result since there was no relief for the tibial crest in the model. Model sensitivity analyses to shank loads showed interface normal and resultant shear stresses were most sensitive to axial force, sagittal bending moment, or sagittal shear force. The finite element model presented in this paper is significant because it contributes toward development of an analytical modeling technique to predict interface stress distributions for proposed prosthetic designs, provides insight into physical explanations of features apparent in interface stress waveforms (thereby enhancing understanding of interface mechanics), and provides insight into nonlinear characteristics that need to be added to improve the model.

Keywords: *amputee interface, finite element modeling, interface stress, prosthetics.*

INTRODUCTION

A prosthetic limb is a common rehabilitation treatment to replace function lost as a result of lower-limb amputation. This treatment places heavy demands on residual limb soft tissues. Rather than supporting the body weight load on the plantar surface of the foot, an amputee is forced to tolerate the entire load of body weight at the interface of the residual limb and the prosthetic socket, an area of skin tissue that is not usually subjected to such intensive magnitudes of normal and shear stress. Possible skin responses to these high stresses are: 1) an inflammatory response followed by necrosis and ulceration; or, 2) an adaptation process in which skin becomes durable and load-tolerant. Thus, tissue response to ambulation with a prosthesis can be separated into a two-step process. First, normal and shear stresses are generated at the interface of the residual limb and the prosthetic socket. Second, residual limb tissues respond to interface stresses by either adapting to become load-tolerant or else undergoing an inflammatory response and breaking down.

The first part of this two-step process is addressed in this paper. We have developed an analytical model using the finite element (FE) method that predicts interface normal and shear stresses during ambulation based on characteristics of the amputee, as well as shape and mechanical properties of the prosthesis made by the prosthetist.

The model is an extension of models previously reported in the literature. Linear static models have been developed in order to investigate interface stress distributions during standing and their sensitivity to prosthesis and residual limb characteristics. Pearson's (1) conically-shaped below-knee model analysis used rigid body mechanics to demonstrate that distal cavity pressure was highly sensitive to the interface coefficient of friction. Nissan's (2) short-below-knee stump model was based on cadaver bone geometry measurements and static equilibrium equations. Results from this analysis showed that interface forces were highly sensitive to stump length and socket recesses. More recently, Silver-Thorn (3) found that, under the specific conditions she tested, interface pressure errors determined with a generic geometry FE model were of similar magnitude to those determined from a model with a more accurate representation of residual limb geometry (plaster casts and computer tomography scans), suggesting that model errors were not due to geometric factors, but instead, to material property or boundary condition assumptions. Mak (4) evaluated the adequacy of an elliptical model and an axisymmetric model by comparing interface stress results with those from a 3-dimensional model. Results for the elliptical and axisymmetric models were similar. Quesada (5) developed a finite element model of a below-knee prosthesis of patellar-tendon-bearing design and showed that a 14 percent reduction in interface normal stress at antero-distal and posterior sites was possible with a 10 times reduction in the elastic modulus of the liner material. Winarski (6) demonstrated that there existed a flexion-extension alignment angle that minimized amputee mechanical energy expenditure. Using two test subjects, the investigators demonstrated that this optimal adjustment was very close to the design point set by certified prosthetists.

Krouskop (7), Steege (8), and Torres-Moreno (9) pursued research methodologies that were directed toward incorporating FE models directly into prosthetic design. For Krouskop (for above-knee amputees), and Steege (for below-knee amputees), a user would specify a desired pressure pattern on a residual limb for static alignment conditions, and then a FE model would calculate the socket shape necessary to induce that pressure pattern. Krouskop reported that his model was used 'effectively' to fit two above-knee amputee subjects. Steege's model used constant dilatation elements for tissue as described in detail by Silver-Thorn (10). An iterative removal of constraints was used on surface elements that went into tension. Steege noted that model results were sensitive to tissue stiffness and to underlying tendinous and bony structures of the residual limb. Steege's model is still in a developmental stage; it has not yet undergone clinical evaluation on a population of amputee patients. Torres-Moreno has an above-knee amputee model at a similar developmental stage that shows good correlation between measured standing pressures and model predictions.

The FE model presented in this paper is an extension from previous models in that it addresses interface stresses during ambulation. Ambulation-induced interface stresses are of primary clinical interest because tissue breakdown and the subsequent functional impairment occur more often as a result of ambulation than from standing. Two important simplifying assumptions are made in the model described in this paper: it is quasi-static and it is linear. These assumptions reduce computational intensity, and make it possible to superpose model results for different shank load vectors to generate waveforms for the entire stance phase. Stance phase model results are then compared with stance phase experimental measurements and the following hypotheses are tested:

(i) The model accurately predicts, within instrumentation error, interface stress magnitudes and waveform shapes;

(ii) Model interface stresses are significantly different for a skin moduli of 3.5 kPa compared with a skin moduli of 6.9 kPa;

(iii) Model interface stresses are most sensitive to prosthetic shank axial force, sagittal shear force, and sagittal bending moment, and are relatively insensitive to other force directions in the shank.

By addressing these hypotheses, the model is evaluated, physical understanding of interface me-

chanics is improved, and model characteristics that need or do not need further specification are identified, setting directions for further model development. The long-term goal is an analytical tool that can be used to predict interface stress distributions for proposed socket designs for use in both clinical treatment and prosthetics research.

METHODS

A FE model was developed for one unilateral below-knee amputee subject who underwent interface stress measurement studies at approximately the same time. The subject was 23 years of age, 178 cm tall, 65.9 kg in weight, and had suffered a traumatic injury as the cause of his amputation. He had been an amputee for 4 years and was using a total contact socket of patellar-tendon-bearing design along with Seattle™ System (Model and Instrument Development, Seattle, WA) shank, ankle, and foot components at the time of the study. He regularly used a latex sleeve suspension. By putting a thin layer of powder in the bottom of the socket and then having the subject ambulate, it was demonstrated that he did not distal end-bear: there was no powder transfer to the residual limb. By clinical examination, he had a very bony stump with little soft tissue, especially distally.

The three inputs required for FE model development were determined as follows:

1. *Geometries.* Magnetic resonance (MR) imaging was conducted to determine residual limb tissue geometries. The subject was positioned supine in a 1.5 Tesla magnet (Signa, General Electric) with his residual limb in the same socket used for interface stress measurement. His legs were positioned parallel to each other, and his knees were put in approximately 5 degrees of flexion. The posterior socket surface was supported laterally and posteriorly with foam blocks, taking care to ensure that the supporting load was well-distributed over the posterior socket surface so that minimal bending moment was induced on the residual limb within the socket. Nineteen axial cross-sectional images at 10 mm intervals and 15 coronal images at 12 mm intervals were collected in a 20-minute session. Though only axial images were used for mesh generation, coronal slices were used to ensure that there were not any gross bone or soft tissue abnormalities that were not

apparent in axial images. The resolution of the system in the plane being sampled was 1 mm.

Contours at Pelite™/skin, skin/fat, skin/bone, skin/muscle, and muscle/bone interfaces were digitized from each axial cross-sectional image. The Pelite/hard socket interface was added to the model by generating contours outward normal to the Pelite/skin interface except at the distal end which was left as a free surface since the subject did not distal end-bear. The femur, tibia, and joint capsule were connected together and modeled as a single rigid body. The model was extended proximally partway up the thigh to ensure interface stress results were not affected by conditions at the edge of the model.

A FE mesh totaling 795 nodes and 840 elements was generated. Eight-node isoparametric brick elements were used for skin and fat (SF), muscle, and Pelite materials. Quadrilateral shell elements were used for the socket while beam elements were used for the shank. The bone and knee joint were assumed to be zero displacement surfaces; thus, no elements were generated for them. Evaluation runs were conducted to ensure element edge angles and element face warping were within acceptable levels. Element edge angles were within a 45° to 135° range. Warping factor, defined as (on an element face: distance from the first node to the fourth node parallel to the element normal)/(average thickness of the element) was less than 0.1 for most of the elements and less than 1.0 for all elements. Where necessary, brick elements were degenerated to wedges to ensure acceptable face angles and warping factors. Attempts were made to keep wedge elements to the central muscle region. In high stress gradient regions, evaluation runs with smaller element sizes were conducted to ensure convergence.

2. *Boundary Conditions.* Shank forces and moments were measured using an instrumented pylon (11) at the same time that interface normal and shear stress data were collected. The pylon was a 15.2 cm long 4.1 cm outer diameter aluminum tube with 20 strain-gages mounted in the central 4.5 cm to measure axial force, shear forces, bending moments, and torsional moment. During data collection sessions a 16-channel data acquisition system was used. Twelve channels were used for interface stress measurements (three channels for each of four transducers), leaving four channels available for shank force and moment measurement. In a data

collection session, either the two bending moments or the two shear forces were measured with axial force and torsional moment.

At the proximal end of the model, which was partway up the thigh, zero displacement conditions were specified for bone in the cross-section of the thigh. Soft tissues rested on elastic foundations. Because the proximal end of the model was far from the socket, stump/socket interface stresses were not affected by the zero displacement proximal boundary conditions. Zero displacement conditions were also specified on the surfaces of the tibia, femur, and joint capsule which, as described above, were connected together and specified as a single rigid body. Thus, the knee joint was not allowed to flex or extend over the course of stance phase. This was considered acceptable because the force boundary conditions were specified on the distal end of the model instead of on the proximal end; thus the direction of the applied load relative to the socket was not affected by the lack of knee flexion, and soft tissues were extended sufficiently proximally to avoid edge effects.

3. *Material Properties.* Material properties for SF and muscle were taken from the literature (12,13). Skin has been shown to be nonlinear and anisotropic, with a mechanical response that depends nonlinearly on changes in temperature, humidity, and stress history (12). These nonlinearities, however, were not accounted for in the current model, since computing time limitations required the model to be quasi-static and linear. All materials were assumed linear, homogeneous, and isotropic. A modulus of 5.2 kPa was specified for skin, while a modulus of 131 kPa was specified for muscle. A Poisson ratio of 0.49 was used for all soft tissues.

Material properties of vacuum-formed Pelite were measured experimentally under uniaxial compression. Load-deformation curves were nonlinear at low stress values, but an approximately constant slope of 1.8 MPa was measured at stresses between 20 kPa and 200 kPa. Since interface normal stress measurements were typically between 20 kPa and 200 kPa, a modulus of 1.8 MPa was used in the FE model. A Poisson ratio of 0.39 which was from handbook data was used.

Using the ANSYS® finite element package (Swanson Analysis Systems, Houston, PA), the model was run under unit loads for each of the six shank force and moment directions. Quasi-static

waveforms of the stance phase of gait were generated by superposition. At time t in each waveform:

$$S_{jk}(t) = \sum_{i=1}^{6} (P_i(t)) (U_{ijk})$$

where $S_{jk}(t)$ is stress in direction j at transducer site k, i is one of the six prosthetic shank loading directions, $P_i(t)$ is the measured prosthetic shank load in direction i, and U_{ijk} is interface stress per unit load in direction j at transducer site k for a unit shank load in direction i.

Details of the experimental data collection sessions with which model results in this paper are compared are described in detail elsewhere (14,15). Briefly, interface normal and shear stresses at four sites and four shank forces and moments were measured during walking trials on below-knee amputee subjects. The transducers were custom-designed by the investigators. They measured forces in three orthogonal directions applied to a 6.35 mm diameter sensing surface. The measured forces were divided by the transducer surface area to determine stresses. For biaxial force measurement in the plane of the transducer surface, a 1.5 mm square cross-section beam was instrumented with strain-gages to measure the difference in bending moment between gage sites (**Figure 1**). The beam supported a two-part
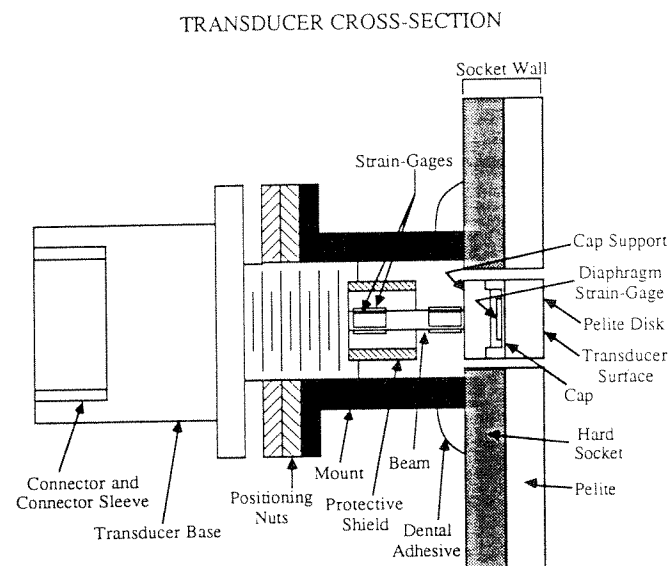
TRANSDUCER CROSS-SECTION

Figure 1.
A cross-sectional view of the transducer used to measure interface stresses in three orthogonal directions in data collection sessions.

short cylinder that was instrumented on its inside top surface with a diaphragm strain-gage. A 6.35 mm diameter disk of Pelite was affixed to the top of the transducer so that no foreign material was introduced to the residual limb. Instrumentation error for the transducers was 4.2 percent full-scale output for the normal direction, and 0.9 percent full-scale output for the shear directions (15).

For the subject data reported in this paper, two data collection sessions were conducted. For the first session, transducers were positioned at antero-lateral proximal, antero-lateral distal, antero-medial proximal, and postero-proximal sites, and prosthetic shank frontal shear force, sagittal shear force, axial force, and torsional moment were measured. In the second session, transducers were positioned at antero-lateral proximal, antero-lateral distal, antero-medial proximal, and postero-distal sites, and prosthetic shank frontal bending moment, sagittal bending moment, axial force, and torsional moment were measured. Subjects walked the length of an 18 m × 1.2 m pathway during a trial to the cadence of a metronome, and data were collected for 8 seconds during each trial. Only steps for which the subject achieved a cadence consistent with the metronome were used in analysis. Typically, the four or five central steps in a trial met this criterion. At least four trials were conducted at each of three angular alignment settings of the socket relative to the shank in the sagittal plane: 'plantarflexion,' 'zero,' and 'dorsiflexion.' The angular adjustments at the alignment jig were 12° for plantarflexion and 4° for dorsiflexion. No translational adjustment was made to accommodate foot displacement.

When comparing analytical data and experimental results, individual steps were analyzed rather than average steps. Because only four shank forces and moment waveforms were collected during a step, however, two shank waveforms needed to be added to each step to achieve a full set of force boundary conditions for the model. Each of the two missing shank waveforms was the average waveform for all steps at the same alignment collected in a different session. Average shank sagittal shear force waveforms for each of three alignments are shown in **Figure 2a**. As shown in the power spectra (**Figure 2b**), the standard deviations were greater for the higher frequency part of the waveform than the lower frequency components, a result found in all six force directions.

SAGITTAL SHEAR FORCE AT THREE ALIGNMENT SETTINGS
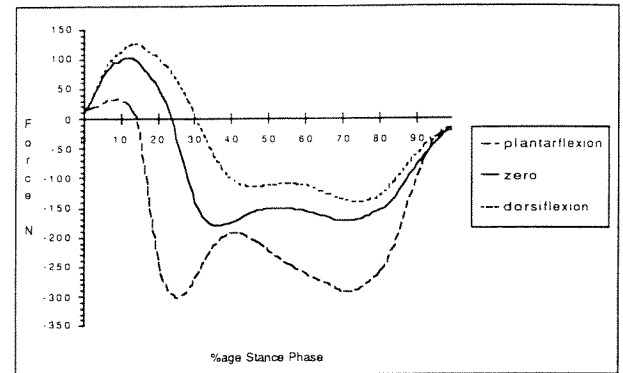
(a)
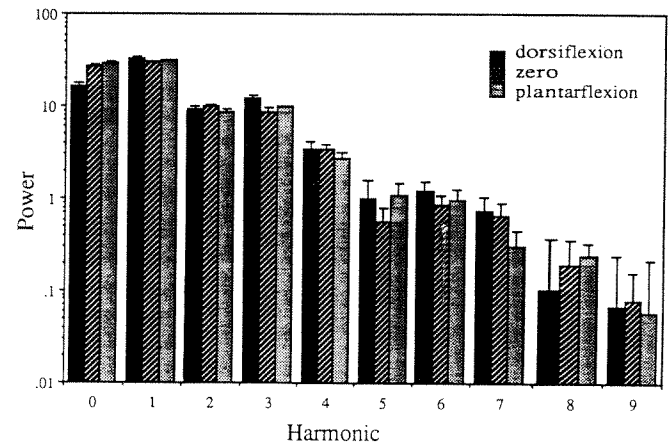
(b)

Figure 2.
(a) Sagittal shear force in the prosthetic shank for three alignment settings: dorsiflexion, zero, and plantarflexion; and *(b)* the corresponding power spectra. Three trials (five steps in each trial) are included for each of the three alignment settings.

Sensitivity Analyses

To evaluate sensitivity to prosthetic shank loading direction, interface stresses were calculated for each shank loading direction separately: *(i)* frontal shear force; *(ii)* sagittal shear force; *(iii)* frontal bending moment; *(iv)* sagittal bending moment; *(v)* axial force; and, *(vi)* torsional moment. Average peak maxima or minima, whichever had a greater absolute magnitude during stance phase, were used for each of the shank loading directions. Those values were -74.3 N, -180.3 N, 7.8 N-m, 55.4 N-m, 818.7 N, and 4.95 N-m for shank loading direction *(i)* to *(vi)* respectively. The coordinate system sign conventions are shown in **Figure 3a** and described below. Thus, the calculation provided an assessment of which shank loading directions most

significantly affected each transducer measurement direction, given the assumption that only maximal magnitude shank loads during stance phase were considered.

To evaluate model sensitivity to tissue material properties, model fits to experimental data were compared for different material property combinations. Model runs were carried out with **E** and **G** specifications listed in **Table 1**, which reflect ranges from the literature (12,13).

RESULTS

The following sign conventions are used for presentation of results. For the prosthesis coordinate system, axial force (z-direction) is positive when directed in the proximal direction, while sagittal shear force (y-direction), and frontal shear force (x-direction) are in the pylon cross-section in sagittal and frontal planes, respectively (**Figure 3a**). An anteriorly directed sagittal shear force on the foot is positive in sign and a laterally directed (right-legged amputee) frontal shear force on the foot is positive in sign. Sagittal bending moment and frontal bending moment are specified with respect to the center of the alignment jig in a sagittal and frontal plane, respectively. Torsional moment is about the shank axis. All moments are positive by a right-hand rule sign convention.

For each transducer, four stresses are defined (**Figure 3b**). 'Normal stress' is perpendicular to the interface, and 'resultant shear stress' is in the plane of the interface. Resultant shear stress is the resultant vector of two components: 1) 'horizontal shear' is in a transverse plane and is positive in the clockwise direction when viewing a socket from above; 2) 'vertical shear' is perpendicular to horizontal shear in the plane of the interface. It is positive when directed distally. Shear stresses ap-plied to the transducers, as opposed to stresses applied to the residual limb, are positive in sign, and compressive stress on the skin is positive.

Comparison of Analytical and Experimental Data

Analytical interface stress curves were usually double-peaked, matching the general trend in clinical data. However, correlation within individual steps varied in quality among sites. Qualitatively, best matches were achieved at postero-distal and antero-proximal sites. Consistent mismatches were seen in antero-lateral distal normal stress waveforms, which became negative partway through stance, and postero-proximal normal stress waveforms, which showed minima instead of maxima at axial force and sagittal shear force first peaks.

Experimental and analytical (Model Case #1, **Table 1**) peak interface stress magnitudes during stance phase were compared. At the zero alignment, the model significantly ($p < 0.05$, t test) underestimated posterior normal stress, antero-medial proximal normal stress, and all resultant shear stresses, except antero-medial proximal resultant shear stress. It significantly ($p < 0.05$) overestimated antero-lateral distal normal stress and antero-lateral proximal normal stress. Differences between peak stress magnitudes for analytical vs. experimental results are shown in **Table 2**. Closest fits were achieved at postero-distal and antero-medial proximal sites. Instrumentation error, which was 4.2 percent full-scale output (FSO) for normal stress and 0.9 percent FSO for shear stress (15), was included in the above significance calculations.

Unlike clinical data (16), analytical data at all sites (except posterior normal stresses), showed significantly ($p < 0.05$) different peak magnitude interface stresses for plantarflexion alignment setting results compared to zero alignment setting results. For dorsiflexion compared to zero alignment set-

Table 1.
Tissue material property combinations used in the analytical model.

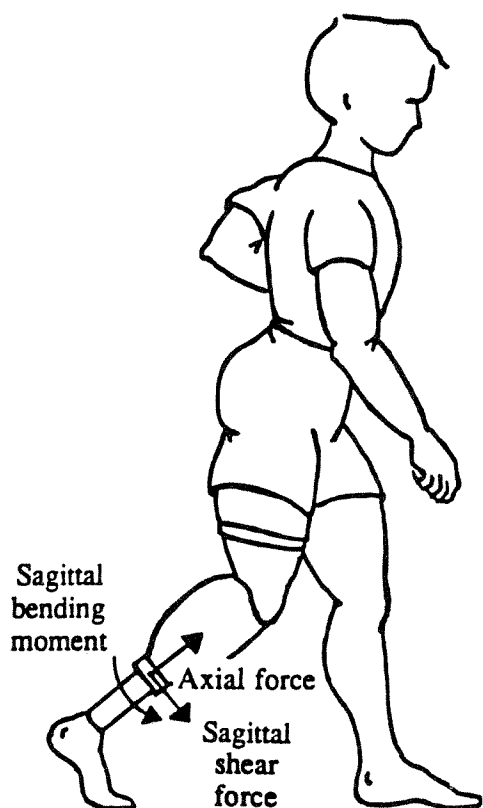| MODEL CASE	E_{skin} (kPa)	G_{skin} (kPa)	E_{muscle} (kPa)	G_{muscle} (kPa)
1	5.2	1.7	131	44.0
2	6.9	2.3	131	44.0
3	3.5	1.2	131	44.0

Figure 3a.
Sign conventions for prosthetic shank sagittal plane shear force, axial force, and sagittal bending moment are shown. The center of the alignment jig is the origin of the coordinate system.

Figure 3b.
Sign conventions for normal stress, horizontal shear stress, vertical shear stress, and resultant shear stress are shown at an antero-lateral distal site. Note that the grid density for this figure is not the FE mesh size.

tings, antero-medial proximal normal stress and antero-lateral proximal resultant shear stress demonstrated significantly (p<0.05) different peak magnitudes, unlike clinical data where no significant difference was demonstrated for any site.

A comparison of resultant shear angles during mid-stance is shown in **Figure 4**. Resultant shear angles were directed more distally in analytical data than in clinical data at all sites. Analytically, the antero-lateral proximal site was the only anterior site not directed toward the midline of the tibia.

Though resultant shear angles did not match quantitatively, changes in resultant shear angle waveform shapes over the course of stance phase were similar in shape for clinical and analytical data (**Figure 5**). Resultant shear angle directions did not show consistent changes for different alignments in either clinical or analytical datasets.

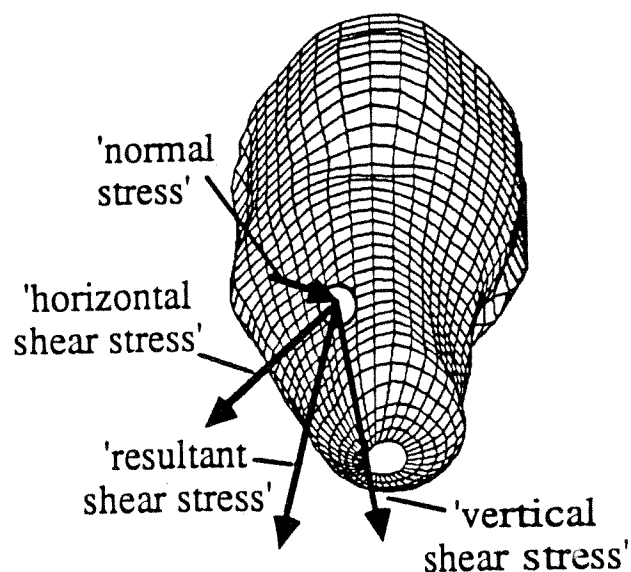In interface stress results from data collection sessions, there were characteristics in the waveforms that were repeated from one step to the next (17). Analytical matches with some of the characteristics of waveform shape are described below.

Loading Delays. 'Loading delays' were times of zero stress at the beginning of interface stress curves (**Figure 6**, first 12 percent of stance phase). They were due to a source other than low shank force and moment magnitudes. At 12 percent into stance phase in the steps shown in **Figure 6**, axial force is at approximately 300 N, more than 30 percent of its maximal value.

FE model data showed loading delays approximately of equal length to those found in clinical data in the same step (**Figure 6**). Exceptions were posterior normal stresses and antero-proximal resultant shear stresses which showed minimal or no loading delays in analytical data, though loading delays were present in experimental results. Also, antero-medial proximal normal stresses in analytical data were often negative during the loading delay phase, a result not found in experimental data.

In the model, loading delays were a result of the shank resultant force being directed antero-proximally. When sagittal shear force and axial force were both positive in sign (which was the case during loading delays, but not later in stance phase),

Table 2.
Comparison of analytical results with experimental data: 'under X%' = underestimated by X%; 'over Y%' = overestimated by Y%.

NORMAL STRESS

	site				
alignment	postero-proximal	antero-medial proximal	antero-lateral proximal	antero-lateral distal	postero-distal
plantarflexion	under 90%	over 49%	over 95%	over 550%	under 16%
zero	under 89%	under 29%	over 63%	over 221%	under 25%
dorsiflexion	under 86%	under 83%	over 52%	over 197%	under 19%

RESULTANT SHEAR STRESS

	site				
alignment	postero-proximal	antero-medial proximal	antero-lateral proximal	antero-lateral distal	postero-distal
plantarflexion	under 82%	under 19%	under 49%	under 51%	under 44%
zero	under 87%	under 11%	under 53%	under 74%	under 51%
dorsiflexion	under 88%	under 1%	under 57%	under 75%	under 54%

sagittal shear force contributed positively, and axial force contributed negatively to all normal stresses except those at posterior sites. Posterior sites were the only sites that did not show analytical normal stress loading delays. Thus, interface stress contributions from sagittal shear force and axial force on anterior interface stresses summed to zero during loading delay phases.

High Frequency Events. High frequency events (HFEs) were maxima or inflection points occurring partway up the rising parts of interface stress curves within the first 40 percent of stance phase. Two types of HFEs were found. Those early in stance, 'early HFEs' occurred within the first 12 percent of stance phase and matched up well with HFEs in shank force and moment waveforms, while those later in stance, 'late HFEs' usually occurred just before the shank resultant force shifted from being directed anterior of the midline to posterior of the midline. Thus, the source of early HFEs was HFEs in the prosthetic shank loads, while the source of late HFEs was a rotational shift in the sagittal plane

of the residual limb within the prosthetic socket. In addition, the dynamic response of residual limb tissues could also have contributed to late HFEs.

Early HFEs were often present in analytical data when present in the corresponding clinical data waveforms, but they were usually not of the same magnitude (**Figure 7a, 7b**). In postero-proximal resultant shear stress, postero-distal resultant shear stress, antero-lateral distal resultant shear stress, and antero-lateral distal normal stress, timings of early HFEs usually corresponded to timings of early HFEs in prosthetic shank axial force and shear force waveforms.

Late HFEs were present in analytical results at some sites, but they were often shifted in time with respect to clinical data. For example, in **Figure 7a** clinical late HFEs occurred later than those in analytical data. **Figure 7b**, however, shows a case where late HFEs occurred simultaneously.

First Peaks. The timing of interface stress maxima occurred at or near the time of the prosthetic shank axial force and sagittal shear force
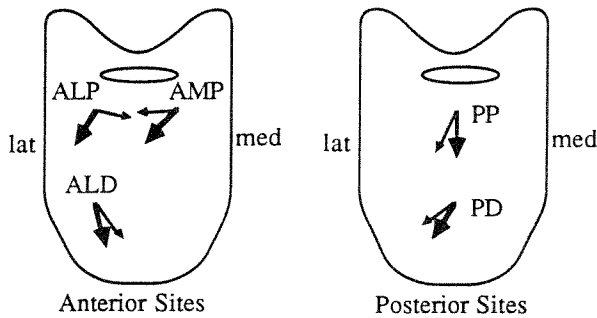
RESULTANT SHEAR ANGLES

Figure 4.
Resultant shear direction on socket surfaces for clinical (thin arrows) and analytical results (thick arrows) during mid-stance. lat = lateral; med = medial.
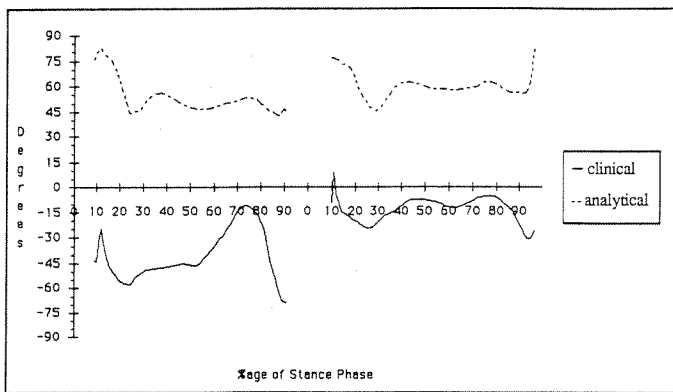
RESULTANT SHEAR ANGLE: ANTERO-MEDIAL PROXIMAL SITE

Figure 5.
Resultant shear angles at an antero-medial proximal site for clinical and analytical data during stance phase are shown from two consecutive steps with a zero alignment setting. Swing phase between the two steps, the first 8% of stance, and the last 8% of stance have been removed for clarity.
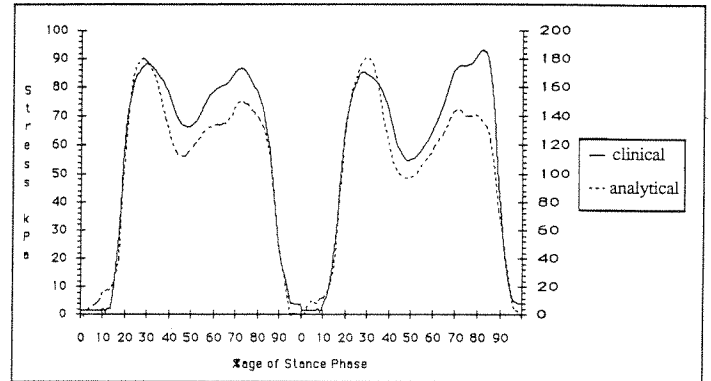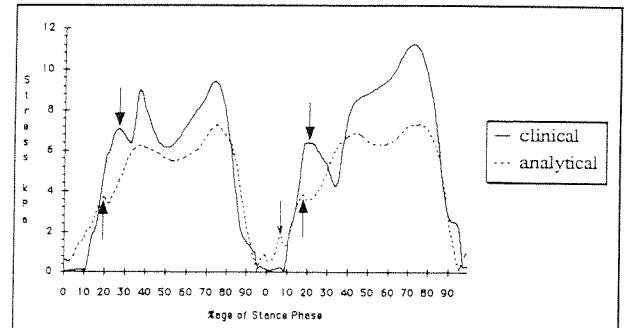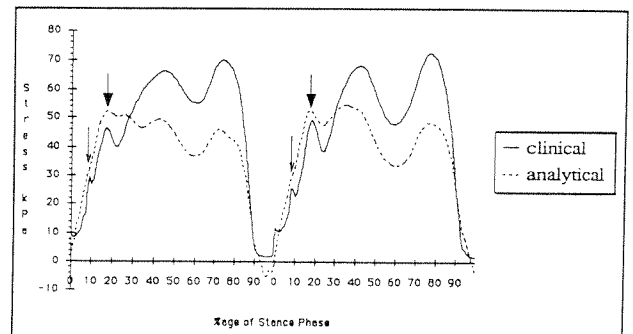
NORMAL STRESS: ANTERO-LATERAL PROXIMAL SITE

Figure 6.
Normal stress at an antero-lateral proximal site during stance phase of two consecutive steps at a plantarflexion alignment setting are shown. Stance phase between the steps has been removed for clarity. The left scale is for clinical data (solid line) and the right scale is for analytical data (dashed line).

RESULTANT SHEAR STRESS: ANTERO-MEDIAL PROXIMAL SITE

(a)

NORMAL STRESS: POSTERO-DISTAL SITE

(b)

Figure 7.
Early HFEs are indicated with thin arrows while late HFEs are indicated with thick arrows. *(a)* Resultant shear stress at an antero-medial proximal site at a plantarflexion alignment setting. *(b)* Normal stress at a postero-distal site at a dorsiflexion alignment setting.

peaks, approximately the same as in clinical data. Exceptions were postero-proximal normal stress, antero-lateral distal normal stress, and antero-lateral distal resultant shear stress which, in model results, had negative slopes or were at minima at axial force and sagittal shear force peaks.

Unlike clinical data, peak magnitudes in the first half of stance phase in analytical results changed for different alignment settings. The following were significantly ($p < 0.05$) lower for the dorsiflexion alignment setting compared with the plantarflexion setting: antero-lateral distal normal stress and resultant shear stress, and antero-lateral

proximal normal stress. Antero-medial proximal resultant shear stress was significantly higher for dorsiflexion vs. plantarflexion alignments.

Central Stance. Model results were usually more underestimated during central stance (i.e., the time between the first and second peaks), compared with the rest of stance phase.

Toe-Off. In analytical data at anterior sites, interface stress waveforms at the antero-lateral distal site showed a maximum or a minimum right before toe-off that was not present in clinical data. This was because in the model, slip was not allowed between the residual limb and socket. Tension was induced during toe-off in skin elements that bordered the interface.

Analytical Model: Sensitivity Analyses

Prosthetic Shank Loading Directions. Analyses were conducted to evaluate sensitivity to prosthetic shank loading directions. **Table 3** shows model interface stress results for maximal magnitude shank loads for each of the six force and moment directions. Thus, the table provides an assessment of which shank loading directions most significantly contributed to horizontal shear, vertical shear, normal, and resultant shear stresses, given the assumption that only maximal magnitude shank forces and moments were considered.

There were several trends apparent (**Table 3**):

1. For all normal and resultant shear stresses, except antero-lateral distally, frontal shear force and frontal bending moment values were low compared to other directions;
2. For all vertical shear stresses, except at the antero-lateral distal site, interface stresses for axial force were at least twice that of any other shank force and moment direction;

Table 3.
Model interface stresses (in kPa) for maximal stance phase loads for each prosthetic shank force and moment direction.

| TRANS-DUCER SITE | STRESS DIRECTION | SHANK LOAD DIRECTION | | | | | | |
		Frontal Shear Force	Sagittal Shear Force	Frontal Bending Moment	Sagittal Bending Moment	Axial Force	Torsion Moment	Total
antero-lateral proximal	horiz shear	0.02	−1.27	0.33	1.41	2.11	2.34	4.94
	vert shear	−1.04	−1.44	−0.59	1.88	6.94	−0.72	5.03
	normal	14.83	36.39	8.58	−37.24	119.24	27.06	168.85
	result shear	−1.04	−1.93	0.68	2.35	7.25	2.45	9.77
antero-lateral distal	horiz shear	1.31	−1.63	0.73	2.89	−3.07	1.14	1.36
	vert shear	1.12	1.90	1.36	−8.42	6.22	−0.21	1.97
	normal	107.19	198.35	71.96	−410.45	97.80	13.29	78.14
	result shear	−1.72	−2.51	1.54	8.90	6.94	1.16	14.30
postero-proximal	horiz shear	−0.30	−0.03	0.07	−0.02	−0.79	1.27	0.20
	vert shear	−0.28	1.08	−0.12	−1.83	5.05	0.09	4.00
	normal	−2.03	−12.68	1.05	5.07	11.62	4.84	7.88
	result shear	−0.41	−1.08	0.14	1.83	5.11	1.27	6.86
postero-distal	horiz shear	0.13	0.43	0.17	−0.91	2.11	0.87	2.79
	vert shear	−0.42	0.52	−0.15	−0.37	3.04	0.18	2.79
	normal	−0.55	−22.58	−0.68	17.17	62.19	−2.44	53.11
	result shear	−0.44	−0.67	0.23	0.99	3.70	0.89	4.69
antero-medial proximal	horiz shear	0.41	−0.16	0.42	0.22	2.18	1.72	4.78
	vert shear	−0.40	−2.32	−0.28	3.01	6.15	−0.72	5.43
	normal	−17.78	55.51	−10.44	−63.90	61.09	−20.39	4.10
	result shear	−0.57	−2.33	0.51	3.02	6.52	1.86	9.01

3. Except at the antero-lateral distal site, normal stresses were most sensitive to axial force, sagittal bending moment, and sagittal shear force. Resultant shear stresses were most sensitive to axial force, sagittal bending moment, and sagittal shear force at antero-lateral distal and antero-medial proximal sites, but were most sensitive to axial force, sagittal bending moment, and torsional moment at antero-lateral proximal, postero-proximal, and postero-distal sites.

It is important to note that the relative proportions of shank force and moment components changed over the course of stance phase. The results in **Table 3** are only an assessment at maximal shank force and moment magnitudes; thus, they were not necessarily reflective of the entire gait cycle.

Tissue Material Properties. Changes in skin material property specifications in the model affected quantitative results, but had minimal effect on shape. When E_{skin} was increased from 3.5 kPa to 6.9 kPa, peak stance phase interface stresses decreased at all but the postero-distal normal stress site. For antero-medial proximal and antero-lateral proximal normal and resultant shear stresses, the average decrease was 7.4 percent (± 1.9 percent), while for postero-proximal and antero-lateral distal stresses, the decrease was 28 percent (± 12.8 percent). Shapes of interface stress waveforms changed more during early stance phase than later in stance phase **(Figure 8)**. It is important to reemphasize that

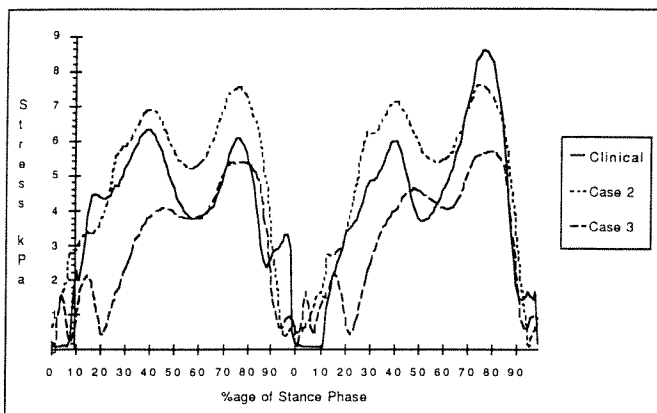RESULTANT SHEAR STRESS: ANTERO-MEDIAL PROXIMAL SITE

Figure 8.
Analytical results for material property Cases 2 and 3 from **Table 1** are compared with clinical data.

linear material properties were specified in the model. To more thoroughly evaluate effects of material properties, a biphasic or multiphasic load-deformation curve would need to be considered and tested using a sensitivity analysis.

DISCUSSION

In the field of lower-limb prosthetics, analytical finite element modeling offers strong potential to make significant contributions to improvement in the treatment and quality of life of individuals who require prosthetic limbs. Stresses at the interface of the residual limb and the prosthetic socket, as well as stresses within the residual limb tissues themselves could, in concept, be predicted by FE models, adding powerful new tools to current clinical techniques of prosthetic design and fitting as well as prosthetics research. Clinicians and researchers would be provided with more information than ever before previously possible about the manifestations of a particular prosthetic design on amputee interface mechanics.

This paper contributes toward this goal by addressing three hypotheses concerning a FE model. The model is quasi-static and linear, and soft tissues are assumed homogeneous and isotropic. Thus, the model is a tremendously simplified representation of the actual residual limb and prosthetic socket and the very fundamental nature of this model should be emphasized. However, it is useful because assessment of the three hypotheses provides insight into aspects of the model that need further development and indicates where further attention should be concentrated.

(i) Hypothesis #1 is false. The model does not accurately predict magnitudes and shapes within the instrumentation error. The four features described below, if added to the model, would improve the match between experimental and analytical data. The basis and justification for selection of the four features is described.

Slip/Loss of Contact. A lack of accounting for slip or loss of contact was a principal cause of several described errors in model fit to experimental data. Because elements were permitted to carry tension across the interface, resultant shear stresses on the skin surface as a whole were underestimated. Strong evidence is provided during the loading delay

phase of stance phase at the antero-medial proximal site which experienced negative normal stress which, from shank sensitivity analyses, was clearly a result of contributions from sagittal bending and sagittal shear forces. Further evidence of the importance of not allowing loss of contact was provided later in the central part of stance phase. Postero-distal and antero-proximal sites matched the best of all transducer sites because the positive sagittal plane bending moment caused them to experience compressive normal stress, unlike the postero-proximal and antero-lateral distal sites which were in much greater error because they experienced tension when under a positive sagittal bending moment. Postero-proximal normal stress, antero-lateral distal normal stress, and antero-lateral distal resultant shear stress in analytical data had negative slopes or were at a minimum at the time of the first peak in experimental data.

Silver-Thorn (10) has described a technique to account for loss of contact across the interface during standing with weight-bearing. An iterative procedure is used whereby tissue interface elements are searched after an analysis run and 'released' if they are in tension in a direction normal to the interface. The analysis is then repeated with the new boundary conditions. Such a procedure could be used to study interface stresses during ambulation, though each datapoint in a stance phase waveform would need to be analyzed independently because unit load results could no longer be superposed, adding considerable computation time to the analysis. Another alternative would be to specify springs at the interface with different properties in tension and compression.

Material Nonlinearities. The assumption that soft tissues and Pelite behaved mechanically as linear materials was another source of error in the model. An approximately biphasic stress-strain curve would be a more accurate description of skin mechanical response. In the model presented in this paper, only the first slope portion of the curve was modeled and interface stress sensitivity to the modulus investigated. Further modeling efforts with a nonlinear load-deformation curve should investigate interface stress sensitivity to the second slope and to the location of the 'elbow' at the intersection of the first and second linear portions. The location of the 'elbow' has been shown to be highly sensitive to age (18) which is related to elastin content, thus for modeling of residual limbs tissues the location of the 'elbow' would be expected to be sensitive to body location and orientation and the presence of scar tissue. In addition, attachments between tissue layers must be considered. On the anterior residual limb surface, skin is adherent to underlying fascia, thus under moderate shear loading on the skin surface, stress concentrations within the skin would be expected to be induced. On the posterior surface, however, skin slides over underlying fascia. In addition, the deep fascial layer beneath the skin is characterized by a high in-plane stiffness (19), but a low in-plane bending stiffness. In posterior tissues, the fascia layer would be expected to redistribute concentrated normal stress so that muscle and connective tissue within the compartments surrounded by fascia experience a uniform stress distribution. Skin has also been shown to be sensitive to stress history, though after a few repeated cycles, load-deformation curves become repeatable (12). Anisotropic characteristics have been demonstrated in animal skin (20), though the degree of anisotropy depends on the location. Thus, appropriate further directions in model development are to evaluate interface stress sensitivity to the shape of material property curves, anisotropy, connections between tissue layers, and interface properties.

Pre-Stresses. A modeling error related to material nonlinearities is the assumption of initial total contact and zero pre-stress between the residual limb and the prosthetic socket. Slight geometry differences between the actual and modeled residual limbs are not important as demonstrated by Silver-Thorn (3). Instead, it is the manifestations of geometry mismatching between the residual limb surface and the socket surface on skin pre-stresses that is important. Slight pre-stress will cause a shift in the 'elbow' region of the biphasic load-deformation curve for skin toward the origin which would be expected to drastically alter subsequent interface stress distributions generated during gait. Thus, nonlinear tissue and interface material property specifications as described above would allow this hypothesis to be tested. The initial total contact specified in the model is an explanation for error between analytical and experimental resultant shear directions on anterior surfaces. There was no socket relief for the tibial crest in the model; thus there was a high interface normal stress on the tibial crest.

Measurement of All Shank Components Simultaneously. The effects of adding two shank loads that were not measured during the steps being modeled was to effect the shapes of model interface stress results. Mismatches in the timings of high-frequency content events (i.e., loading delays and HFEs) were apparent. As shown in **Figure 2b**, the low-frequency content of prosthetic shank waveforms changed minimally for different steps; however, the high-frequency content changed appreciably. To overcome these problems, a modified prosthetic force and moment measurement system is being constructed at the University of Washington to measure all six shank components simultaneously.

(ii) Hypothesis #2 is false. Model interface stresses were significantly different for a skin modulus of 3.5 kPa compared with a skin modulus of 6.9 kPa. It should be noted however, that changes at postero-proximal and antero-lateral distal sites were greater than those at antero-proximal locations. Skin modulus in the antero-proximal area was not as highly sensitive a parameter as at postero-proximal and antero-lateral distal sites. It is important to note that linear material properties were assumed. Further investigation using nonlinear tissue material specifications as described above are needed to verify the finding of low sensitivity.

(iii) Hypothesis #3 is false. While it is true that all normal stresses and some resultant shear stresses were most sensitive to prosthetic shank axial force, sagittal bending moment, and sagittal shear force, it was demonstrated that resultant shear stresses at postero-distal, postero-proximal, and antero-lateral proximal sites were more sensitive to torsion than to sagittal shear force. Low posterior site sensitivity is expected because the peak stance phase sagittal shear force is directed posteriorly, which unloads posterior sites. Because the antero-lateral proximal site was oriented such that the normal direction was parallel with the sagittal plane, resultant shear stresses at the antero-lateral proximal site were minimally sensitive to sagittal shear force.

Both normal stresses and resultant shear stresses were minimally sensitive to frontal shear force and frontal bending moment, suggesting that those directions have minimal influence on interface stress magnitudes. Further investigation using the nonlinear tissue and interface properties described above need to be conducted to verify this finding. In addition, it should be noted that possibly other parameters important to fit (such as stability and comfort) are affected by the frontal shear and frontal bending values.

In addition to evaluation of the three hypotheses presented in this paper and identification of necessary parameters to consider in future modeling efforts, analytical model results also provide insight into an understanding of interface mechanics, adding useful knowledge applicable to clinical treatment. Effects on interface mechanics of loading delays, alignment, and material property sensitivity are described below.

Two sources of the loading delays were hypothesized previously (17): 1) slip at the interface; and, 2) a manifestation of the antero-proximally directed shank resultant force vector. Because data from the analytical model, which did not allow for slip at the interface, demonstrated loading delays, it is concluded that direction of the anterior resultant force vector played a significant role in generating loading delays. Loading delays are important because if they end at uneven times on the residual limb, skin will be put in tension (14), a potentially detrimental stress configuration.

As supported by the results presented here **(Table 2)**, the lack of a change in interface stress magnitudes for different alignment settings is not necessarily exclusively a result of differences in shank loading combinations. Instead, a factor not accounted for in the model, such as the residual limb being aligned differently with respect to the socket surface, a change in the amount of slip at the interface, or a change in residual limb muscle activation, was responsible.

Sensitivity analyses to tissue material properties showed that interface stresses were lower if material properties on both sides of the interface were more closely matched. Skin/liner interface stresses were reduced if the modulus difference between the skin and liner was reduced. It should be noted, however, and it is certainly recognized clinically, that amputee gait stability will also be affected by material properties. Thus, they should also be considered when selecting properties for liner materials.

ACKNOWLEDGMENTS

REFERENCES

1. Pearson JR, Grevsten S, Almby B, Marsh L. Pressure variation in the below-knee patellar tendon bearing suction socket prosthesis. J Biomech 1974:7:487-96.
2. Nissan M. A simplified model for the short-below-knee stump. J Biomech 1977:10:651-8.
3. Silver-Thorn MB, Childress DS. Use of a generic, geometric finite element model of the below-knee residual limb and prosthetic socket to predict interface pressures. In: Proceedings of the Seventh World Congress of the International Society of Prosthetics and Orthotics. Chicago: 1992:272.
4. Mak AFT, Hong ML, Chan C. Finite element models for analyses of stresses within above-knee stumps. In: Proceedings of the Seventh World Congress of the International Society of Prosthetics and Orthotics. Chicago: 1992:147.
5. Quesada P, Skinner HB. Analysis of a below-knee patellar tendon-bearing prosthesis: a finite element study. J Rehabil Res Dev 1991:28(3):1-12.
6. Winarski DJ, Pearson JR. Least-squares matrix correlations between stump stresses and prosthesis loads for below-knee amputees. J Biomech Eng 1987:109:238-46.
7. Krouskop TA, Muilenberg AL, Doughtery DR, Winningham DJ. Computer-aided design of a prosthetic socket for an above-knee amputee. J Rehabil Res Dev 1987:24(1):1-8.
8. Steege JW, Silver-Thorn MB, Childress DS. Design of prosthetic sockets using finite element analysis. In: Proceedings of the Seventh World Congress of the International Society of Prosthetics and Orthotics. Chicago: 1992:273.
9. Torres-Moreno R, Solominidis SE, Jones D. Load transfer characteristics at the socket interface of above-knee amputees. In: Proceedings of the Seventh World Congress of the International Society of Prosthetics and Orthotics. Washington, DC: 1992:274.
10. Silver-Thorn MB. Prediction and experimental verification of residual limb/prosthetic socket interface pressures for below-knee amputees. (Dissertation). Evanston, IL: Northwestern University, 1991.
11. Sanders JE. Ambulation with a prosthetic limb: mechanical stresses in amputated limb tissues. (Dissertation). Seattle, WA: University of Washington, 1991.
12. Daly CH. The biomechanical characteristics of human skin. (Dissertation). Glasgow, Scotland: University of Strathclyde, 1966.
13. Shock RB, Brunski JB, Cochran GVB. In vivo experiments on pressure sore biomechanics: stresses and strains in indented tissues. 1982 Advances in Bioengineering. Thibault L, ed. 1982:88-91.
14. Sanders JE, Daly CH, Burgess EM. Interface shear stresses during ambulation with a prosthetic limb. J Rehabil Res Dev 1992:29(4):1-8.
15. Sanders JE, Daly CH. Measurement of stresses in three orthogonal directions at the residual limb/prosthetic socket interface. IEEE Trans Rehabil Eng 1993:1(2). In press.
16. Sanders JE, Daly CH, Burgess EM, Boone DA. Interface mechanics: effects of alignment change. In: Proceedings of the Seventh World Congress of the International Society of Prosthetics and Orthotics. Chicago: 1992:370.
17. Sanders JE, Daly CH, Burgess EM. Clinical measurement of normal and shear stresses on a transtibial residual limb: characteristics of waveform shape during walking. Prosthet Orthot Int 1993:17:38-48.
18. Daly CH, Odland GF. Age-related changes in the mechanical properties of human skin. J Invest Dermatol 1979:73:84-7.
19. Gratz CM. Tensile strength and elasticity tests on human fascia lata. J Bone Joint Surg 1931:13:334-40.
20. Lanir Y, Fung YC. Two-dimensional mechanical properties of rabbit skin—II. Experimental results. J Biomech 1974:7:171-82.